Čerenkov-type second-harmonic generation with fundamental beams of different polarizations

Yan Sheng,[1] Solomon M. Saltiel,[2,3,†] Wieslaw Krolikowski,[3] Ady Arie,[4] Kaloian Koynov,[1,*] and Yuri S. Kivshar[3]

[1]*Max-Planck Institute for Polymer Research, Ackermannweg 10, 55128 Mainz, Germany*
[2]*Faculty of Physics, University of Sofia, 5 J. Bourchier Boulevard, 1164 Sofia, Bulgaria*
[3]*Nonlinear Physics Center and Laser Physics Center, Center for Ultra-high Bandwidth Devices for Optical Systems (CUDOS), Research School of Physics and Engineering, Australian National University, Canberra, Australian Capital Territory 0200, Australia*
[4]*Department of Physical Electronics, School of Electrical Engineering, Tel-Aviv University, Tel Aviv 69978, Israel*
**Corresponding author: koynov@mpip-mainz.mpg.de*

Received December 7, 2009; revised February 23, 2010; accepted February 24, 2010; posted March 10, 2010 (Doc. ID 120677); published April 20, 2010

We analyze the conical second-harmonic generation via Čerenkov-type phase matching in two-dimensional decagonal nonlinear photonic quasi-crystals for linear, circular, and elliptical polarized fundamental beams. Depending on the polarization state, we observe either centrosymmetric or noncentrosymmetric intensity modulation of the second-harmonic rings. We explain this effect by employing the concept of effective quadratic nonlinearity combined with the hexagonal symmetry of the individual ferroelectric domains. © 2010 Optical Society of America

OCIS codes: 190.2620, 190.4420, 220.4000, 050.1940.

Second-harmonic generation (SHG) is one of the most known parametric processes in nonlinear optics. It can be achieved by a variety of ways depending on the phase matching, polarizations of the interacting waves, and the type of a nonlinear medium. One of the most interesting schemes is the Čerenkov-type SHG [1], named so because of the close analogy with the famous Čerenkov effect when a charged particle traveling faster than the speed of light in the medium emits conical radiation [2]. Similarly, in the case of the Čerenkov SHG, the second-harmonic (SH) signal is observed as a conical wave defined by the longitudinal phase matching condition $k_2 \cos\theta - 2k_1 = 0$, where θ is the Čerenkov angle [see Fig. 1(a)]. While the demonstrations of the Čerenkov SHG in bulk nonlinear crystals have been reported [1,3,4], this type of SHG is more often realized in the waveguide geometry [1] because of higher light intensities [5–8].

Nonlinear quadratic photonic crystals (NQPCs) are structures with spatial modulation of the nonlinear susceptibility $\chi^{(2)}$, and they create a new class of materials providing a valuable platform for the study of the light-matter interactions in a nonlinear regime [9–12]. While the Čerenkov-type SHG in one-dimensional (1D) NQPC made of potassium titanyl phosphate was reported several years ago [13], the effect was attributed to $\chi^{(2)}$ of domain walls, since the symmetry of the crystal forbids bulk emission of the SH in the investigated geometry. We have recently demonstrated the Čerenkov SHG via bulk $\chi^{(2)}$ tensor component in 1D $LiNbO_3$ [14] and two-dimensional (2D) $LiTaO_3$ and $LiNbO_3$ NQPCs [15,16]. We found that the modulation of $\chi^{(2)}$ in NQPCs greatly enhances the intensity of the Čerenkov emission. This effect is preserved in materials with randomized domains, as evident from the Čerenkov SHG observed in $Sr_xBa_{1-x}Nb_2O_6$ and $Ca_xBa_{1-x}Nb_2O_6$ crystals [17,18]. In this Letter we analyze, both experimentally and theoretically, the dependence of the Čerenkov SHG in NQPCs on the polarization state of the fundamental beam. In contrast to all previous studies [13–15,17,18] that were performed with linearly polarized fundamental waves, we investigate the Čerenkov SHG in a 2D quasiperiodic NQPC using fundamental beams of linear, circular, and elliptical polarizations. We find a strong dependence of the azimuthal intensity modulation of the Čerenkov-like SH rings on the input polarization. This effect can be explained by employing the concept of the effective nonlinearity $d_{\text{eff}}^{(2)}$ combined with the hexagonal symmetry of individual ferroelectric domains. We derive simple equations that describe the dependence of $d_{\text{eff}}^{(2)}$ on the fundamental beam polarization.

Our experimental setup is depicted in Fig. 1(b). The fundamental beam is provided by a mode-locked Nd:YAG laser that delivers 30 ps 1 mJ pulses at 1064 nm with a repetition rate of 10 Hz. The beam is di-

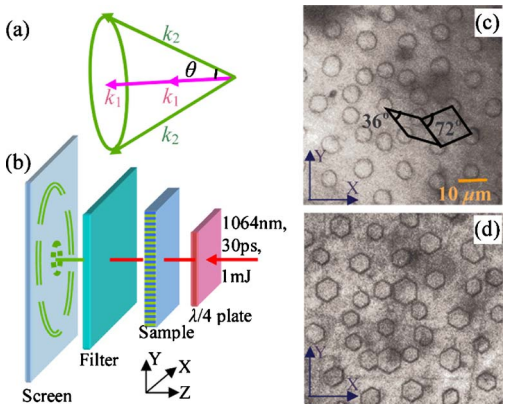

Fig. 1. (Color online) (a) Phase-matching condition for Čerenkov-type SHG. (b) Schematic of the experiment. (c), (d) Micrographs of the quasiperiodic domain structures at the $\pm Z$ surfaces, respectively.

 © 2010 Optical Society of America

rected normal to the crystal surface and focused to a spot size of ≈500 μm in the plane of the crystal. Its polarization can be continuously varied by rotating a $\lambda/4$ plate. After passing through the sample the fundamental beam is blocked by appropriate filters, and the emitted SH signal is projected onto a screen and recorded using a CCD camera. The 2D NQPC used is a quasiperiodically poled $LiNbO_3$ crystal (thickness of 0.4 mm) whose lattice is created by tiling the plane with two types of rhombi: "thin," with vertex angles of 36°, and "thick," with vertex angles of 72° and placing the inverted domains in the corners of the rhombi. The side length of the rhombi is 13.19 μm, and the diameter of the inverted domains is 5 μm. The tiling is done using the inflation-deflation method (self-similar transformation) and well described by the Penrose model [19,20]. The ferroelectric domain patterns obtained by etching the $\pm Z$ surfaces of the NQPC are shown in Figs. 1(c) and 1(d). While the reversed domains are circular at the $+Z$ surface, they acquire hexagonal shape at the $-Z$ surface owing to the $3m$ symmetry of the $LiNbO_3$ crystal [21]. Both surfaces ($\pm Z$) of the NQPC were polished for the Čerenkov SHG experiments.

Figure 2(a) shows the SH emission patterns recorded with fundamental beams of different polarizations (from left to right: linear, elliptical, circular, and elliptical). Two Čerenkov-type SH rings with close diameters, corresponding to cone angles of 40.0° and 38.0°, are clearly seen in all cases. Inside the rings, close to the center there is an additional SH structure that is a result of a Raman–Nath-type nonlinear diffraction [14,15]. As illustrated in Fig. 3, the two Čerenkov SH rings are orthogonally polarized. While the internal ring is polarized radially, the polarization of the external ring is azimuthal. Since the fundamental wave is always ordinary the internal ring is a result of an E_2-O_1O_1 interaction, and the external one is a result of an O_2-O_1O_1 interaction. Using the dispersion data for $LiNbO_3$ [22] and the phase matching equations, $\sin\beta_o = n_{2,o}\sin[\cos^{-1}(2k_{1,o}/k_{2,o})]$ and $\sin\beta_e = n_{2,e}\sin[\cos^{-1}(2k_{1,o}/k_{2,e})]$, we calculate the Čerenkov angles $\beta_o = 40.08°$ and $\beta_e = 38.06°$. These

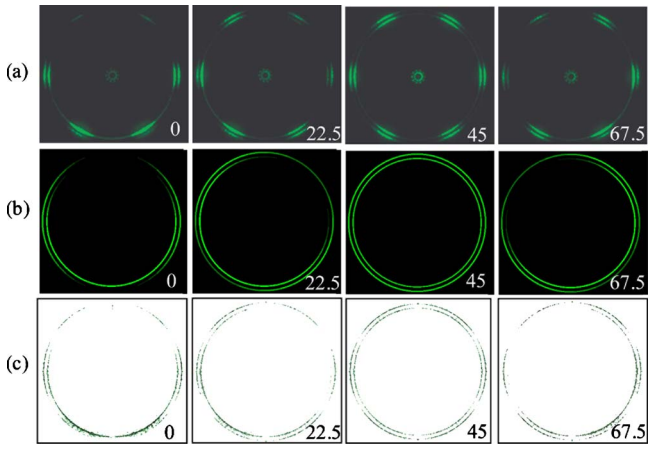

Fig. 2. (Color online) (a) Experimentally recorded and (b), (c) theoretically predicted Čerenkov SH rings with fundamental beams of different polarizations. The angles marked in the figure correspond to δ in Eqs. (1) and (2).

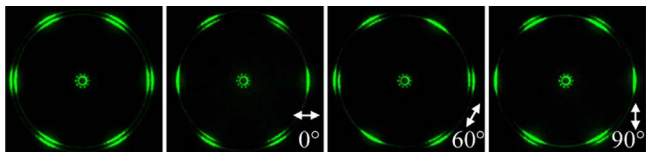

Fig. 3. (Color online) Polarization properties of the Čerenkov SH rings. From left to right images are taken without analyzer, analyzer oriented horizontally, analyzer at 60°, and analyzer oriented vertically. The input beam is circularly polarized.

values agree well with our experimental results (40.0° and 38.0°).

Unlike the Čerenkov angles that are not sensitive to the fundamental polarization, the azimuthal intensity distribution of the Čerenkov rings changes significantly upon the variation of the fundamental polarization. As seen in Fig. 2(a), the pattern transforms gradually from noncentrosymmetric into centrosymmetric when the fundamental beam polarization is varied from a linear to circular polarized beam. In all cases, however, an additional sixfold azimuthal modulation is observed. Furthermore, while the relative intensities of the six maxima change with the input polarization, their positions depend only on the orientation of the $LiNbO_3$ crystal. Rotation of the sample by some angle leads to rotation of the sixfold structure by the same angle.

The dependence of the Čerenkov ring azimuthal modulation on the fundamental beam polarization is determined by the polarization-dependent $\chi^{(2)}$ term. As explained above, the inner Čerenkov ring is generated by an E_2-O_1O_1 interaction, and the outer ring by an O_2-O_1O_1 interaction. $d_{\text{eff}}^{(2)}$ for these processes can be written as

$$d_{\text{eff}}^{(o)} = d_{22}[\cos(\varphi + 2\gamma) - i\,\sin 2\delta \sin(\varphi + 2\gamma)], \quad (1)$$

$$d_{\text{eff}}^{(e)} = d_{32}\sin\theta_e \cos 2\delta + d_{22}\cos\theta_e \times[\sin(\varphi + 2\gamma) + i\,\sin 2\delta\cos(\varphi + 2\gamma)], \quad (2)$$

where φ is the azimuthal angle, γ defines the direction of the fast axis of the $\lambda/4$ plate (they are both measured counterclockwise from the X axis of the $LiNbO_3$ crystal), and δ is the angle between the $\lambda/4$ plate and the polarization plane of the Nd:YAG laser (see Fig. 4).

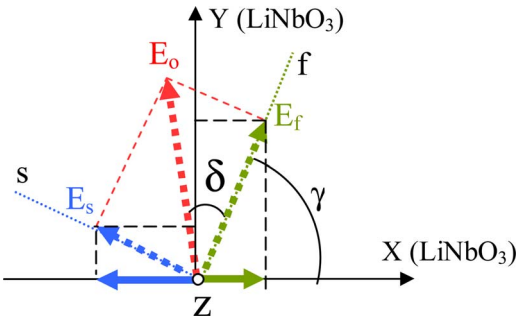

Fig. 4. (Color online) Definitions of the angles and vectors for the derivation of the effective nonlinearities.

For weak focusing and negligible pump depletion the SH intensity is directly proportional to $|d_{\mathrm{eff}}^{(2)}|^2$. In Fig. 2(b) we plot the Čerenkov SH intensity distributions, $I_2^{(o,e)}=A|d_{\mathrm{eff}}^{(o,e)}|^2$, where A is a constant and $d_{32}/d_{22}=-3.9$ [23]. It can be seen that the SH rings have constant intensities at all azimuthal angles only for the circularly polarized fundamental beam. For all other polarization states, the SH intensities change gradually with the azimuthal angle. The outer ordinary SH rings have two intensity maxima (minima), and the inner extraordinary SH rings have only one intensity maximum (minimum). A comparison of Figs. 2(a) and 2(b) shows that the $d_{\mathrm{eff}}^{(2)}$ approach describes very well the effect of the fundamental polarization on the azimuthal intensity distribution of the Čerenkov rings. This simple theoretical model, however, does not explain the experimentally observed sixfold modulation of the SH rings. To understand this modulation one should consider that, besides $d_{\mathrm{eff}}^{(2)}$, the SH intensity also depends on the Fourier coefficient g_i associated with the reciprocal vector $\mathbf{G}_i$. For a circular shape of the individual inverse domains, the Fourier spectrum $\{g,\mathbf{G}\}$ is represented by the first-order Bessel function [24], which is radially symmetric in the 2D reciprocal space. However, in our samples the domains have a hexagon shape, as clearly shown in Fig. 1(d). The actual Fourier spectrum reflects this hexagonal symmetry, resulting in a sixfold azimuthal modulation of the SH intensity, I_2. As we have shown recently, this effect can be described quantitatively using the following equation [16]:

$$I_2^{(o,e)}(\varphi)=A|d_{\mathrm{eff}}^{(o,e)}|^2|g(\varphi)|^2L^2\left(\frac{\sin[(|G|-\Delta k)L/2]}{(|G|-\Delta k)L/2}\right)^2,$$

where L is the thickness of the sample and $\Delta k=k_2\sin\theta$. This formula is used to calculate the images shown in Fig. 2(c), which includes both the hexagonal intensity modulation and polarization properties of $d_{\mathrm{eff}}^{(o,e)}$, and agrees well with the experiments [Fig. 2(a)].

Finally, we would like to point out that the Čerenkov SHG in our NQPC has a broad acceptance bandwidth for tuning crystal temperature. Furthermore, the observed SH emission patterns change little with the temperature. Indeed, while the Čerenkov angle is determined by the refractive indices of the crystal and varies slightly with the temperature, the amplitude of this variation in the $LiNbO_3$ crystal is too small to be experimentally resolved [22].

In conclusion, we have studied the Čerenkov-type SHG in a 2D quasiperiodically poled $LiNbO_3$ crystal with fundamental beams of linear, elliptical, and circular polarizations. We have observed that the input polarization state has a strong effect on the azimuthal modulation of the Čerenkov SH rings. We have explained this result by employing the concept of $d_{\mathrm{eff}}^{(2)}$ combined with the hexagonal symmetry of individual ferroelectric domains. We believe that the studied effects may be important in the development of several applications such as nondestructive testing of the domain structures, SH microscopy, or the studies of dispersion and polarization properties of the $\chi^{(2)}$ tensor.

We thank Ch. Bubeck and D. Neshev for helpful discussions, A. Best for technical assistance, and acknowledge support from Max-Plank Society, Chinese Academy of Science (CAS), and Australian Research Council.

†Solomon M. Saltiel is deceased.

References

1. A. Zembrod, H. Puell, and J. Giordmaine, Optoelectronics (London) **1**, 64 (1969).
2. J. V. Jelley, *Čerenkov Radiation* (Pergamon, 1958).
3. A. A. Kaminskii, H. Nishioka, K. Ueda, W. Odajima, M. Tateno, K. Sasaki, and A. V. Butashin, Quantum Electron. **26**, 381 (1996).
4. V. Vacaitis, Opt. Commun. **209**, 485 (2002).
5. P. K. Tien, R. Ulrich, and V. Berger, Appl. Phys. Lett. **17**, 447 (1970).
6. K. Hayata, K. Yanagawa, and M. Koshiba, Appl. Rev. Lett. **56**, 206 (1990).
7. M. J. Li, M. de Micheli, Q. He, and D. B. Ostrowsky, IEEE J. Quantum Electron. **26**, 1384 (1990).
8. Y. Zhang, Z. D. Gao, Z. Qi, S. N. Zhu, and N. B. Ming, Phys. Rev. Lett. **100**, 163904 (2008).
9. V. Berger, Phys. Rev. Lett. **81**, 4136 (1998).
10. N. G. R. Broderick, G. W. Ross, H. L. Offerhaus, D. J. Richardson, and D. C. Hanna, Phys. Rev. Lett. **84**, 4345 (2000).
11. Y. Sheng, J. Dou, B. Ma, B. Cheng, and D. Zhang, Appl. Phys. Lett. **91**, 011101 (2007).
12. T. Ellenbogen, N. Voloch-Bloch, A. Ganany-Padowicz, and A. Arie, Nature Photon. **3**, 395 (2009).
13. A. Fragemann, V. Pasiskevicus, and F. Laurell, Appl. Phys. Lett. **85**, 375 (2004).
14. S. M. Saltiel, D. N. Neshev, W. Krolikowski, O. Bang, A. Arie, and Y. Kivshar, Opt. Lett. **34**, 848 (2009).
15. S. M. Saltiel, D. N. Neshev, W. Krolikowski, R. Fisher, A. Arie, and Y. S. Kivshar, Phys. Rev. Lett. **100**, 103902 (2008).
16. S. M. Saltiel, Y. Sheng, N. Bloch, D. N. Neshev, W. Krolikowski, A. Arie, K. Koynov, and Y. S. Kivshar, IEEE J. Quantum Electron. **45**, 1465 (2009).
17. R. Fisher, S. M. Saltiel, D. N. Neshev, W. Krolikowski, and Y. S. Kivshar, Appl. Phys. Lett. **89**, 191105 (2006).
18. P. Molina, S. Alvarez-Garcia, M. O. Ramirez, J. Garcia-Sole, L. E. Bausa, H. Zhang, W. Gao, J. Wang, and M. Jiang, Appl. Phys. Lett. **94**, 071111 (2009).
19. R. Penrose, Bull. Inst. Math. Appl. **10**, 266 (1974).
20. Y. Sheng, J. Dou, J. Li, B. Cheng, and D. Zhang, Appl. Phys. B **87**, 603 (2007).
21. Y. Sheng, T. Wang, B. Ma, E. Qu, B. Cheng, and D. Zhang, Appl. Phys. Lett. **88**, 041121 (2006).
22. D. H. Jundt, Opt. Lett. **22**, 1553 (1997).
23. A. Ganany, A. Arie, and S. M. Saltiel, Appl. Phys. B **85**, 97 (2006).
24. Y. Sheng, J. Dou, J. Li, B. Ma, B. Cheng, and D. Zhang, Appl. Phys. Lett. **91**, 101109 (2007).